**Proceedings of the Canadian Society for Mechanical Engineering International Congress 2021**
**CSME Congress 2021**
**June 27-30, 2021, Charlottetown, PE, Canada**

# Development of an attitude determination and control system for the LORIS CubeSat

Annalisa Wailand[1], Robert Bauer[1*]
[1]Department of Mechanical Engineering, Dalhousie University, Halifax, Canada
[*]robert.bauer@dal.ca

***Abstract***— The Low Earth Orbit Reconnaissance Imagery Satellite (LORIS) is a 2U Earth-observation CubeSat in development at Dalhousie University. This paper describes the proposed attitude determination and control system (ADCS) for this CubeSat. Attitude determination is carried out using the Quaternion ESTimation (QUEST) algorithm in combination with an extended Kalman filter that propagates an internal dynamic model of the CubeSat. A control approach is then proposed that cycles between reaction wheel nadir-pointing control during portions of the orbit when a Sun vector can be estimated, and magnetic detumbling for reaction wheel desaturation during portions of the orbit where Earth eclipses Sun. Computer simulations are then presented to validate the proposed ADCS.

***Keywords-attitude determination; CubeSat; attitude control***

## I. INTRODUCTION

The Dalhousie University Low Earth Orbit Reconnaissance Imagery Satellite (LORIS) is a 2U CubeSat with a dual camera payload to photograph Earth while in low-Earth orbit (LEO). The proposed attitude determination and control system (ADCS) for LORIS features two sets of actuators – three orthogonal magnetorquers and three orthogonal reaction wheels – and a standard suite of sensors including Sun sensors, a magnetometer, and a gyroscope. The LORIS mission requires an attitude determination accuracy of ±10° while the satellite is in view of Sun and a nadir-pointing attitude accuracy of ±10° to be assumed and maintained as quickly as possible once the satellite exits eclipse.

Kalman filtering algorithms can be used to provide estimates of the satellite's attitude quaternion and attitude rates. Quadrino [1], for example, uses magnetometer, Sun and Earth horizon sensor measurements with the TRIAD method [2] to calculate an estimate of the attitude quaternion. This attitude quaternion estimate is then passed into an extended Kalman filter (EKF), along with attitude rates from gyroscope measurements. Furthermore, Soken and Sakai [3] use TRIAD with an unscented Kalman filter (UKF) to estimate attitude and calibrate the magnetometers. While Soken and Sakai [3] and Quadrino [1] propagate the state using kinematics equations of motion, Yang and Zhou [4] found that incorporating spacecraft dynamics into an EKF produces more accurate attitude quaternion estimates. The EKF formulation proposed by Yang and Zhou [4] uses a reduced quaternion model with quaternion measurements and optional gyroscope measurements. They indicate that these quaternion measurements can be obtained using analytical methods [5] or the Quaternion ESTimation (QUEST) method [6]. Esteban *et al.* [7] use QUEST with an EKF that propagates a dynamic model without gyroscope measurements and successfully used this attitude determination approach on their launched nanosatellite INTA-NanoSat-1B. The proposed attitude determination approach for LORIS uses QUEST with an EKF that propagates a dynamic model and incorporates gyroscope measurements.

An important consideration when reaction wheels are present in the system is the incorporation of momentum unloading into the operational plan. Over time, reaction wheels accumulate momentum which will eventually cause the wheels to reach their maximum speed. One momentum dumping solution is to activate magnetorquers simultaneously with the reaction wheels to continuously reduce the excess momentum [8]. This method allows the wheels to operate over longer periods of time and has been demonstrated on the CubeSat scale in simulation [9, 10]. Another momentum dumping solution is to allow the ADCS system to run as planned while tracking the reaction wheels' momentum and, once the momentum passes a specified threshold, activate a separate operational mode that allows the wheels to desaturate. This solution has been used, for example, onboard the x-ray observatory Chandra [11] and the nanosatellite Aoba VELOX-IV [12]. The proposed momentum dumping method for LORIS uses the eclipse portion of each orbit to command the reaction wheels to de-spin while using the magnetorquers to attenuate the satellite body rates.

This paper provides an overview of the ADCS proposed for LORIS and presents the results of computer simulations carried out to validate the proposed approach. Section II describes the space environment implemented in the simulator, Section III explains the proposed attitude determination method, Section IV outlines the magnetic detumbling and nadir-pointing control approach, Section V presents simulation results, and Section VI draws conclusions.

## II. SIMULATION ENVIRONMENT

The ADCS computer simulation tool developed in MATLAB/Simulink utilises the Simscape Multibody Toolbox

The authors received financial support from the Canadian Space Agency (CSA) Canadian CubeSat Project and the Natural Sciences and Engineering Research Council of Canada (NSERC).

to model the satellite's attitude dynamics based on an imported SolidWorks assembly model of the CubeSat. The developed simulation tool assumes perfect orbit determination knowledge based on a two-body acceleration-based orbit propagator model without orbital perturbations. Reference models for Earth's magnetic field and the position of Sun are provided by the International Geomagnetic Reference Field (IGRF) Simulink block and a simplified Sun ephemeris model [13]. Disturbance torques are modelled to reflect the anticipated worst-case environmental torques. The ability of the proposed ADCS control approach to reject these disturbances was then evaluated.

### A. *Worst-Case Disturbance Torques*

The predominant disturbance torques perturbing a satellite's attitude in LEO are gravity gradient, atmospheric drag, solar radiation pressure, and residual magnetic dipole moment. The maxima calculated in this research for these four disturbances are reported in Table I for a nominal nadir-pointing attitude [14].

TABLE I. WORST-CASE DISTURBANCE TORQUES

| Disturbance Torque | Variable | Maximum Value |
|---|---|---|
| Gravity Gradient | $T_{GG}$ | $2.08 \times 10^{-10}$ Nm |
| Aerodynamic Drag | $T_D$ | $1.94 \times 10^{-7}$ Nm |
| Solar Radiation Pressure | $T_{SRP}$ | $7.99 \times 10^{-9}$ Nm |
| Magnetic Dipole Moment | $T_M$ | $5.14 \times 10^{-7}$ Nm |
| Total | $T$ | $7.16 \times 10^{-7}$ Nm |

For the assumptions used in this research, magnetic dipole moment and aerodynamic drag are the dominant disturbance torques. For an Earth-oriented vehicle, the magnetic dipole moment torque is cyclic with a profile mirroring that of the local magnetic field, while the aerodynamic drag torque maintains a constant profile [15]. Sample profiles of the vector components ($T_x$, $T_y$, $T_z$) of the summation of the four disturbance torques over one orbit are shown in Figure 1.

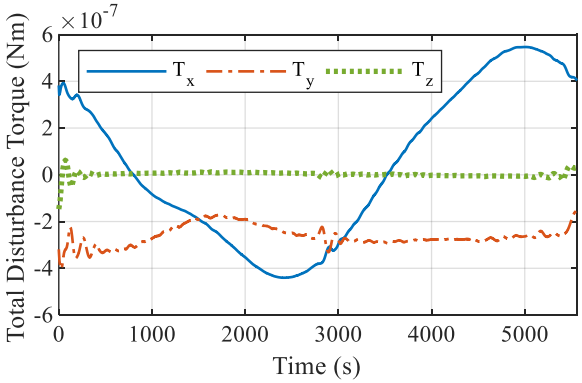


Figure 1. Sum of worst-case disturbance torques ($T_x$,$T_y$,$T_z$) over one orbit

## III. ATTITUDE DETERMINATION

Attitude is defined by the coordinate transformation between the body-fixed (BF) reference frame – fixed along the satellite's principal axes of inertia – and the nadir-pointing (NP) reference frame representing the desired nadir-pointing attitude of the satellite. Both frames have their origins at the satellite's centre of mass, with the NP +Z axis pointing towards Earth's centre as depicted in Figure 2. Reference vectors used to compute satellite attitude are defined with respect to the standard Earth-centred inertial (ECI) reference frame.

The attitude determination component of the LORIS ADCS includes eighteen photodiode Sun sensors and one inertial measurement unit (IMU) containing a three-axis micro electro-mechanical gyroscope and a three-axis digital magnetometer. The relatively high number of Sun sensors was chosen to improve the estimation of the Sun vector in the presence of shadows cast by the solar arrays. In simulation, white Gaussian noise was generated to match the noise variance observed in experiments for similar sensors. This noise was imposed upon the simulated models for each sensor. Using a sample rate of one second, measurements from the magnetometer and Sun sensors are used with QUEST to obtain an initial approximation of the attitude quaternion before passing this quaternion estimate to an EKF for refinement. The EKF provides the basis for the error measurement needed by the CubeSat's nadir-pointing controller.

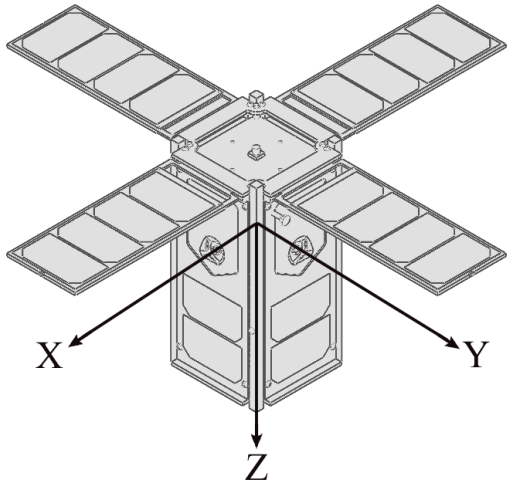


Figure 2. LORIS CubeSat body-fixed reference frame [16]

### A. *QUEST with EKF*

The attitude determination method implemented in the simulator uses the QUEST algorithm first proposed by Shuster in 1981 [6] in combination with an EKF. QUEST calculates an optimal attitude quaternion from the eigen decomposition of a matrix constructed from two different sets of vectors – two measurement vectors in the BF frame and two reference vectors in the ECI frame. The eigenvector corresponding to the maximum eigenvalue defines the optimal attitude quaternion. The two vector sets used in the simulator are the estimated BF Sun vector from Sun sensor readings with the ECI reference Sun ephemeris vector, and the measured BF local magnetic field vector with the ECI reference IGRF magnetic field vector.

The EKF and its internal attitude dynamics CubeSat model expands the reduced quaternion model proposed by Yang [4] to include all four elements of the attitude quaternion [14]. Inputs to the EKF include the estimated attitude quaternion from QUEST, attitude rate measurements from a three-axis gyroscope, reaction wheel torques and reaction wheel speeds. The EKF internal dynamic model presently used in the simulator assumes that the three reaction wheels are situated coincident at the satellite's centre of mass. Both the satellite inertia matrix and the reaction wheel inertia matrix are assumed to be diagonal, and 10% model inertia uncertainty is added to the EKF internal dynamic model.

Three limitations of QUEST likely to cause control issues were discovered during simulator development. The present authors' solution to each limitation involves the use of the EKF attitude prediction in tandem with the calculated attitude quaternion from QUEST. The first issue concerns the availability of sensor measurements and how attitude is handled when it cannot be estimated. For example, when too few Sun sensors are illuminated, a Sun vector cannot be obtained from QUEST. In this circumstance, all four elements of the QUEST quaternion are set to zero to flag the EKF downstream to omit the update phase such that only the prediction phase of the EKF is implemented.

The second issue with QUEST is that the attitude quaternion is not determinable when either the two measurement vectors or the two reference vectors approach parallel. To solve this issue, the present authors set a threshold such that when the input vectors are within 10° of being parallel to one another (i.e. >170° or <10°), all four elements of the QUEST quaternion are set to zero which, as with the first solution, flags the downstream EKF to omit the update phase.

The third issue with QUEST relates to the duality property of the quaternion where a quaternion and its negative counterpart represent equivalent orientations. Figure 3 illustrates this duality issue by comparing the scalar $q_s$ and vector ($q_x$,$q_y$,$q_z$) components of the attitude quaternion calculated by QUEST to the components of the actual attitude quaternion calculated by Simscape. The QUEST quaternion appears to "flip" indiscriminately between the two quaternion solutions – the flipped portions clearly being the negative of the non-flipped portions. This problem with QUEST has also been observed by Campos and Furtado [17]. They propose a solution based on use of the second derivative of the quaternion scalar element to attempt to identify discontinuities in the quaternion output signal. In their solution, if the second derivative of the scalar is greater than some threshold, then a point filter inverts the output until the next discontinuity is detected [17]. Campos and Furtado note that there are limitations with their solution when noise is added to the system [17]. The present authors therefore sought a solution that does not require taking the derivative of a noisy signal.

The solution proposed is a logic condition that compares the QUEST attitude quaternion output against the attitude quaternion estimate from the EKF. As shown in Figure 4, if the 2-norm of the difference between the QUEST quaternion and EKF prediction is greater than the 2-norm of the difference between the negative QUEST quaternion elements and EKF prediction, then the QUEST quaternion is flipped. Referring to Case 1 in Figure 4, the difference between the QUEST quaternion element and EKF quaternion element is smaller than the difference between the negative QUEST and EKF quaternions, and thus the QUEST estimate would not be flipped. For Case 2 in Figure 4, however, the difference between the QUEST quaternion component and EKF quaternion component is larger than the difference between the negative QUEST and EKF quaternions, and thus the QUEST estimate would be flipped.

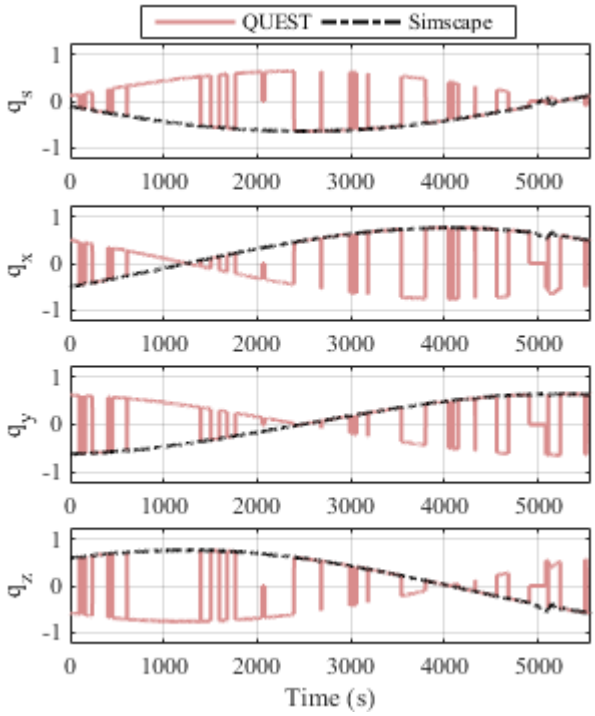


Figure 3. Illustration of quaternion duality problem

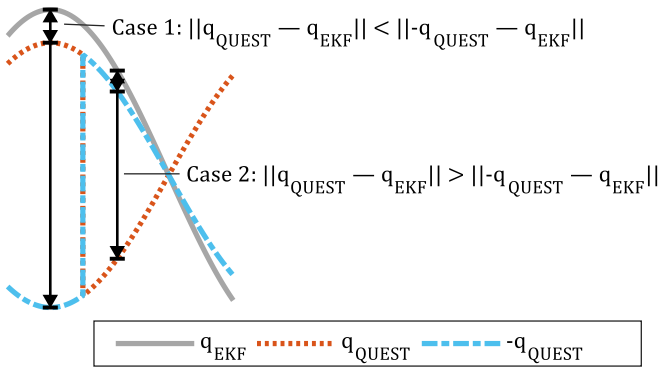


Figure 4. Proposed quaternion duality solution logic condition

Figure 5 compares the raw QUEST attitude quaternion components from noisy sensor data with with the quaternion components predicted by the EKF when all three solutions are implemented. It can be seen in this figure that the proposed solutions work well even in the presence of sensor noise.

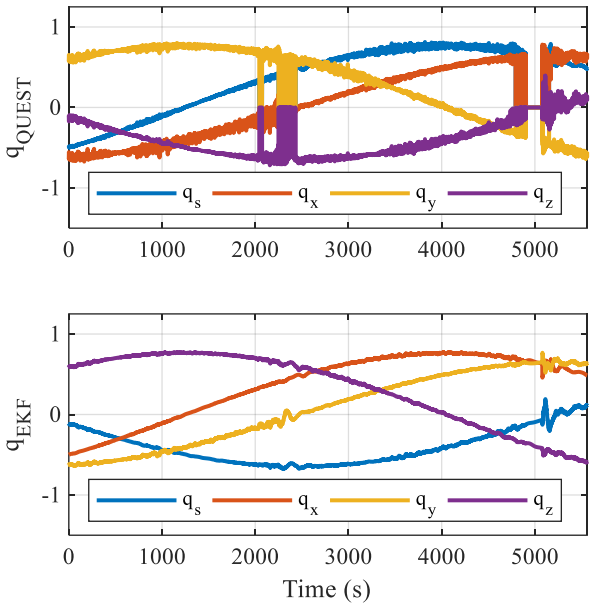


Figure 5. Comparison between the QUEST attitude quaternion components and the EKF attitude quaternion components over one orbit with all three solutions implemented

## IV. Attitude Control

The LORIS ADCS actuators include three magnetorquer rods arranged orthogonally and a reaction wheel system consisting of three orthogonally-oriented reaction wheels. A conservative duty cycle of 90% is applied as a square wave to any magnetic input torque signals in Simulink. This duty cycle allows for any residual magnetic field and consequent residual dipole moment to dissipate before further magnetic field measurements are taken.

### A. B-Dot Detumbling Control

The B-dot algorithm describes a proportional controller that acts on the rate of change of the local magnetic field $\dot{\boldsymbol{B}}$ expressed in the BF frame. This control law determines the desired magnetic dipole moment $\boldsymbol{m}$ in units of $Am^2$ commanded to the magnetorquers based solely on three-axis magnetometer data. The scalar gain $K$ applies a restoring moment about the desired axis to the rotating spacecraft such that [18]:

$$\boldsymbol{m} = -K\dot{\boldsymbol{B}} \tag{1}$$

For a sample time $t_s$ of 1 second, the rate of change of the local magnetic field can be approximated at timestep $k$ from the difference between the current and previous ($k$–1) magnetometer measurements:

$$\dot{\boldsymbol{B}}_k = \boldsymbol{B}_k - \boldsymbol{B}_{k-1} \tag{2}$$

Because magnetic field measurements from magnetometers is generally noisy, an infinite impulse response (IIR) low-pass filter is applied to the calculated derivative to produce a cleaner derivative estimate using the following equation [19]

$$\dot{\boldsymbol{B}} = \alpha\, \dot{\boldsymbol{B}}_k + (1 - \alpha)\, \dot{\boldsymbol{B}}_{k-1} \tag{3}$$

where the smoothing factor $\alpha = 0.03$ was selected empirically to produce the most consistent results.

### B. Proportional Derivative Pointing Control

Pointing control is achieved using a proportional derivative (PD) controller, where the proportional scalar gain $K_p$ acts on the vector portion of the EKF-estimated attitude quaternion error $\hat{\boldsymbol{q}}$ and the derivative scalar gain $K_d$ acts on the EKF-estimated angular rate error vector $\boldsymbol{\omega}$ [20]. The controller computes a reaction wheel motor voltage vector $\boldsymbol{V}_c$ that drives the reaction wheels:

$$\boldsymbol{V}_c = -K_p\hat{\boldsymbol{q}} - K_d\boldsymbol{\omega} \tag{4}$$

Tuning results for the B-dot and PD controllers can be found in [14].

### C. Control Scheme

During nominal satellite operation, the satellite is set to detumble and de-spin the reaction wheels during eclipse and point towards Earth during periods of Sun. In reference to the control scheme layout shown in Figure 6, if the body angular rates exceed a magnitude of 0.04 rad/s or the reaction wheel speeds exceed 5000 RPM at any given time, then the reaction wheels de-spin and the satellite is detumbled until the body rates and wheel speeds fall below these thresholds. Once they do, the availability of the Sun vector is checked. If the Sun vector is available, then the satellite attitude is estimated by the QUEST algorithm which is used in the update phase of the EKF. The updated EKF attitude quaternion estimate is used with the reaction wheel PD controller, and the reaction wheels maintain the satellite in its desired nadir-pointing attitude. If the Sun vector becomes unavailable (either due to eclipse or due to shadows cast by the solar arrays) and QUEST is therefore unable to provide the EKF with an attitude quaternion, then only the prediction phase of the EKF is used to continue providing estimates of the CubeSat's attitude. A 300 second threshold is selected as the average amount of time over which the EKF prediction phase can propagate the internal model to produce a viable attitude estimate without an updated attitude quaternion from QUEST. Once 300 seconds have passed without a Sun vector, the EKF states and the reaction wheel motor voltages are zeroed, the magnetic detumbling B-dot controller is switched on, and the journey through the logic tree in Figure 6 resets.

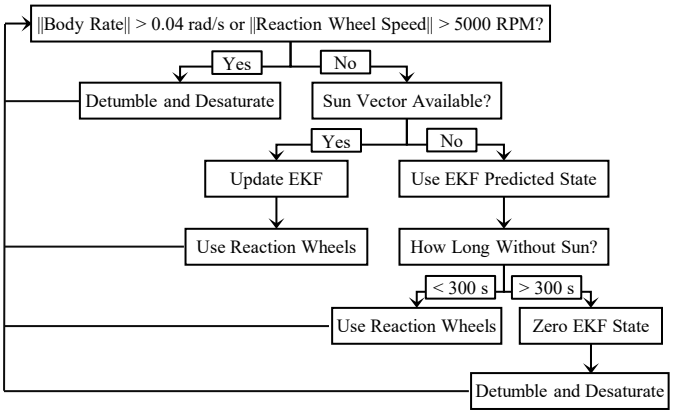


Figure 6. Control switch logic flowchart

As a result of this control approach, the reaction wheels desaturate during every eclipse period and a dedicated momentum unloading mode of operation is not required. If the ADCS is turned back on after a period where the satellite has been in safe mode, it will automatically detumble until any residual body angular rates from this period have been reduced to within the 0.04 rad/s threshold. The CubeSat will then automatically regain its nadir-pointing attitude once Sun is in view. The control scheme effectively detumbles the satellite for all but 300 seconds of every eclipse period, leaving most of the Sun period available for pointing. This solution enables the payload cameras to take daytime photographs of Nova Scotia's shorelines and surrounding waters.

## V. Results

Results were obtained in simulation using orbital parameters derived from a two-line element set for the International Space Station orbit. Table II lists the Simscape model parameters used for the preliminary simulations of the LORIS CubeSat shown in Figure 1. The satellite inertia matrix is assumed to be diagonal, with products of inertia set to zero.

TABLE II. Satellite Mass Properties

| Parameter | Variable | Value |
|---|---|---|
| Mass | $m$ | 1.79 kg |
| Principal Moments of Inertia | $I_x$ | 0.0158 kgm$^2$ |
| | $I_y$ | 0.0158 kgm$^2$ |
| | $I_z$ | 0.0159 kgm$^2$ |
| Centre of Mass | $CoM$ | [0.0197 -0.0247 0.0785] m |

Under the simplifying assumption that the satellite is viewing its target any time the reaction wheels are active, Figure 7 plots the resulting viewing time as a percentage of each orbit over 100 orbits. The theoretical percent maximum viewing time per orbit is 62% – equivalent to the period where the satellite is in Sun. This maximum is marked as a grey-dashed line in Figure 7. The average viewing time per orbit over 100 orbits is 57%, with a maximum viewing time of 62%, a minimum viewing time of 36%, and a standard deviation of approximately 6%. Only 10 orbits of the 100 orbits simulated have less than 50% of their duration available for viewing. The orbits with the largest reduction in viewing time correspond to those orbits where the Sun vector is unavailable for the greatest period of time or those orbits that exceed the body angular rate threshold coming out of eclipse – conditions that often occur in tandem.

Attitude determination error is assessed by taking the quaternion product of the inverse EKF estimated quaternion and the Simscape actual quaternion. This error quaternion is then subsequently converted into its axis-angle representation and the angle component is taken as the attitude determination error. Figure 8 plots the resulting average attitude determination error per orbit over 100 orbits and considers only the periods of the orbit when the satellite is in Sun. An overall average attitude determination accuracy of 2.6 ± 1.1° was computed from the mean data shown in Figure 8, which lies well within the LORIS attitude determination requirement of ±10°.

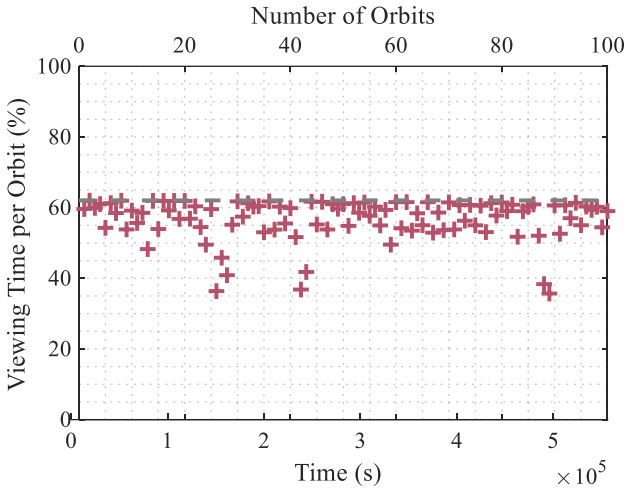


Figure 7. Percent viewing time per orbit for 100 orbits

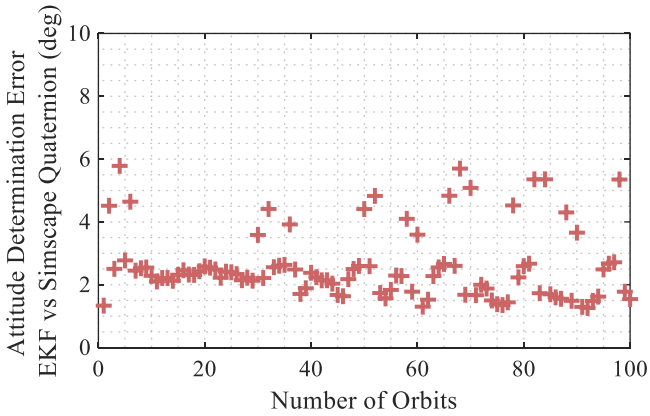


Figure 8. Average attitude determination accuracy per orbit for 100 orbits

Pointing error is assessed over the same 100 orbits in terms of the Euler angles. To simplify computation, the satellite is considered to be pointing after 800 seconds have elapsed post-eclipse. Figure 9 plots the average errors in terms of Euler angles (where $\phi$ = roll, $\theta$ = pitch, and $\psi$ = yaw) for each of the 100 orbits. Standard deviations of the pointing errors are calculated excluding any outlier orbits with average pointing errors greater than 15 degrees about any axis (which excludes only 6% of the simulated orbits). The average pointing error per orbit in terms of Euler angles were computed as $\phi = 1.9 \pm 1.5°$ $\theta = 3.4 \pm 1.1°$ and $\psi = 2.1 \pm 1.8°$. The absolute pointing error was then determined from the angle component of the axis-angle representation of the above set of Euler as 4.4 ±2.7°. This absolute pointing error satisfies the LORIS mission requirement of an attitude pointing accuracy of at least ±10°, achieving nearly double the required degree of accuracy on average.

## VI. Conclusions

This paper presents computer simulation results for the proposed attitude determination and control system for the LORIS CubeSat. For the simulation conditions used in this research an orbit-averaged attitude determination accuracy of 2.6 ± 1.1° was achieved using a determination approach that applies the QUEST method to produce an attitude quaternion

estimate which is subsequently refined by an EKF. By using a reaction wheel PD controller during periods of Sun, and a B-dot detumbling controller during eclipse to regulate reaction wheel speeds, an orbit-averaged absolute pointing accuracy of 4.4 ±2.7° was achieved. Both accuracies lie well within their respective mission requirements of ±10°.

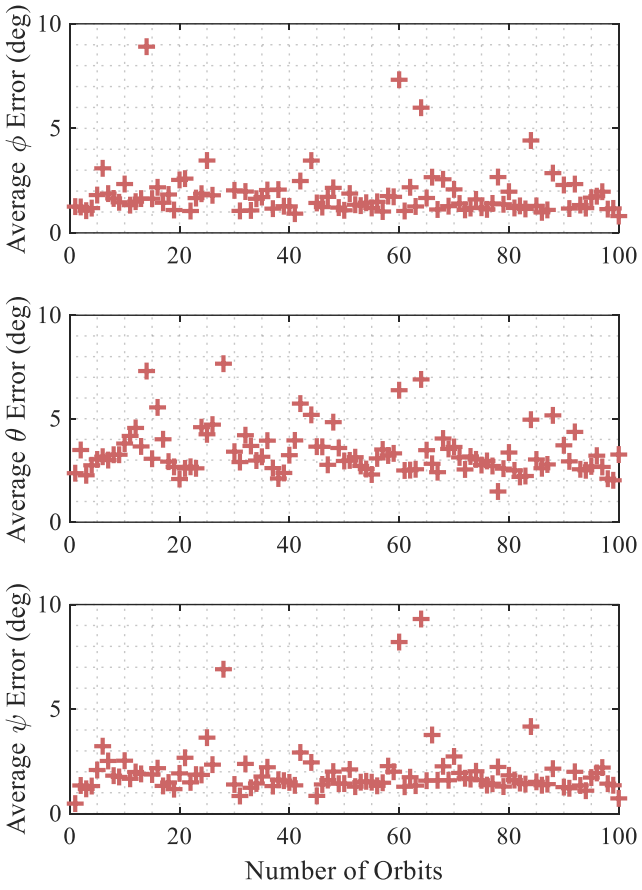


Figure 9. Average pointing accuracy in terms of Euler angles per orbit for 100 orbits

## ACKNOWLEDGMENT

The authors would like to thank the members of the Dalhousie Space Systems Lab for all of their help and support.

## REFERENCES

[1] M. K. Quadrino, "Testing the attitude determination and control of a CubeSat with hardware-in-the-loop", Masters Thesis, Massachusetts Institute of Technology, 2014.

[2] F. L. Markley, "Fast quaternion estimation from two vector measurements", Journal of Guidance, vol. 25, no. 2, 2002, pp. 411-414.

[3] H. E. Soken and S. Sakai, "TRIAD+Filtering Approach for Complete Magnetometer Calibration" in 2019 9th International Conference on Recent Advances in Space Technologies, Istanbul, Turkey, 2019.

[4] Y. Yang, Z. Zhou, "Spacecraft dynamics should be considered in Kalman filter attitude estimation", 26th AAS/AIAA Space Flight Mechanics Meeting, Napa, CA, 2016.

[5] Y. Yang, Z. Zhou, "An analytic solution to Wahba's problem", Aerospace Science and Technology, Vol. 30, 2013, pp. 46-49.

[6] M. D. Shuster and S. D. Oh, "Three-axis attitude determination from vector observations," Journal of Guidance and Control, vol. 4, no. 1, pp. 70-77, 1981.

[7] S. Esteban, J. M. Girón-Sierra, Ó. R. Polo, and M. Angulo, "Signal Conditioning for the Kalman Filter: Application to Satellite Attitude Estimation with Magnetometer and Sun Sensors," Sensors, vol. 16, no. 11, 2016.

[8] P. J. Camillo and F. L. Markley, "Orbit-averaged behavior of magnetic control laws for momentum unloading," Journal of Guidance and Control, vol. 3, no. 6, pp. 563-568, 1980.

[9] E. Oland and R. Schlanbusch, "Reaction wheel design for CubeSats," in 2009 4th International Conference on Recent Advances in Space Technologies, Istanbul, Turkey, 2009.

[10] N. S. Krishna, S. Gosavi, S. Singh, et al., "Design and implementation of a reaction wheel system for CubeSats," in 2018 IEEE Aerospace Conference, Big Sky, MT, 2018.

[11] M. Juda, M. Baski, C. Eagan, et al., "Updating Chandra High-radiation Safing in response to changing observatory conditions," in Proc. SPIE 8448, Observatory Operations: Strategies, Processes, and Systems IV, Amsterdam, Netherlands, 2012.

[12] J. R Alarcon, N. C. Örger, S. Kim, L. K. Soon, and M. Cho, "Aoba VELOX-IV attitude and orbit control system design for a LEO mission applicable to a future lunar mission," in 67th International Astronautical Congress, Guadalajara, Mexico, 2016.

[13] F. L. Markley and J. L. Crassidis, "Fundamentals of spacecraft attitude determination and control", New York, NY: Springer Science + Business Media, 2014, pp. 420-422.

[14] A. Wailand, "Development of a computer simulation tool to study the attitude determination and control of CubeSats", Masters Thesis, Dalhousie University, 2020.

[15] W. J. Larson and J. R. Wertz, "Space Mission Analysis and Design, 2nd ed.", Microcosm, Inc. and Kluwer Academic Publishers, 1992.

[16] Dalhousie Space Systems Lab Chassis Subsystem, CAD Assembly V3.7, 2020.

[17] L. J. E. Campos and E. C. Furtado, "Analysis of quaternions components in QUEST algorithm - the duality problem," in Proceedings of the XXXVIII Iberian Latin-American Congress on Computational Methods in Engineering, Florianópolis, Brazil, 2017.

[18] T. W. Flatley, W. Morgenstern, A. Reth and F. Bauer, "A B-dot acquisition controller for the RADARSAT spacecraft," in Flight Mechanics Symposium, Greenbelt, MD, 1997.

[19] M. N. Nounou and B. R. Bakshi, "Multiscale methods for denoising and compression," in Data Handling in Science and Technology Volume 22, Amsterdam, The Netherlands, Elsevier Science Publishers B.V., 2000, pp. 119-150.

[20] N. Sugimura, T. Kuwahara and K. Yoshida, "Attitude determination and control System for nadir pointing using magnetorquer and magnetometer," in 2016 IEEE Aerospace Conference, Big Sky, MT, 2016.